Grooves Accelerate Dew Shedding

Pierre-Brice Bintein, Henri Lhuissier, Anne Mongruel, Laurent Royon, Daniel
Beysens

Editors' Suggestion   **Featured in Physics**

Grooves Accelerate Dew Shedding

Pierre-Brice Bintein,[1] Henri Lhuissier,[2,3] Anne Mongruel,[3] Laurent Royon,[1] and Daniel Beysens[3,*]

[1]*University Paris Diderot, CNRS, Sorbonne Paris Cité, Laboratoire Interdisciplinaire des Energies de Demain, 75013 Paris, France*
[2]*Aix Marseille Univ, CNRS, IUSTI, 13453 Marseille, France*
[3]*Physique et Mécanique des Milieux Hétérogènes, CNRS, ESPCI, PSL Research University, Sorbonne Université, Sorbonne Paris Cité, 75005 Paris, France*

Gravity-driven drainage of small volumes of condensates, such as natural dew, is a challenge because small drops usually remain pinned to inclined surfaces. We report that submillimetric grooves substantially reduce dew retention by modifying the repartition of liquid: Because of a long-range coalescence mechanism mediated by grooves imbibition, the growth and shedding of large drops are accelerated. Such findings can be applied to increase the passive harvesting of dew as well as to accelerate the drainage of other condensates.

Introduction.—The rising water scarcity [1–3] makes its unconventional sources more attractive [4–6]. Among them, dew water—that is, atmospheric water condensing on surfaces radiatively cooled by exposure to clear sky [6–10]—has a maximal surface yield of approximately $0.7 \, \text{L/m}^2$ (i.e., 0.7 mm) per night [10]. This yield requires a surface inclination below $30°$ [11], together with the fast collection of the sessile dew drops before they evaporate at sunrise. Both conditions compete in gravity-driven drainage. Indeed, the shedding of a sessile drop with radius R starts when the gravitational force $\sim \rho g \sin \alpha R^3$, with ρ the liquid density, g the gravity, and α the tilt angle, overcomes the pinning force $\sim \gamma \Delta \cos \theta R$, with γ the surface tension, $\Delta \cos \theta \equiv \cos \theta_r - \cos \theta_a$, and θ_a and θ_r the advancing and receding contact angles, respectively. A critical depinning drop radius follows, [12,13] $R_c \sim (\Delta \cos \theta / \sin \alpha)^{1/2} \ell$, where $\ell = \sqrt{\gamma / \rho g}$ is the capillary length ($\simeq 2.7$ mm for water). Therefore, the dew retention capacity of smooth surfaces (a fraction of ℓ) compares with their yield: Dew collection is limited by the transient stage before the onset of shedding. Previous studies have developed ultrasmooth or micropatterned coated substrates [14–22] which favor drop nucleation and reduce R_c, but these studies have only considered a steady condensation. Here, we focus on the transient regime and study how micro-grooves, inspired by observations of condensation on horizontal grooved surfaces [14,16] and natural organisms living in arid environments [23–25], allow us to reach R_c earlier. Presumably, such microgrooves without chemical coating and manufacturable as one piece of strong material [26] could be made resilient to weathering.

Experiments.—The grooved surfaces are wafers of material A (SiO$_2$, 100 mm large and 0.7 mm thick) textured by standard photolithography with periodic rectangular

ridges of material B (epoxy resin SU-8, MicroChem). Bare wafers (material A, $\theta_a = 35 \pm 5°$, $\theta_r < 5°$) and uniformly coated wafers (material B, $\theta_a = 80 \pm 5°$, $\theta_r = 65 \pm 5°$) are used as reference smooth surfaces. The cleaned and dried tilted substrates (with grooves along the steepest slope direction within $0.5°$) are placed inside a climatic chamber (Weiss WKL 100) with controlled temperature and relative humidity, and cooled by contact with a Peltier thermostat below the dew point (see Fig. 1). Condensation occurs at a constant rate q measured on smooth surfaces, before drops shed, by pressing a hydrophilic stamp against the surface and weighing the water absorbed by imbibition. We also measured q on grooved surfaces by weighing horizontal substrates. The rate q was found to be independent of texturization.

Preliminary findings.—Figure 2 illustrates the influence of grooves by comparing dew formation and coarsening on the two smooth substrates and on 100 μm periodic grooves, for $q = 45$ nm/s (see also movie 1 in Ref. [27]). From the first instants, sessile drops nucleate and grow by diffusion-limited vapor condensation, and by coalescences. At short times, the drop populations on the three substrates are spatially uniform because the drops size is smaller than the
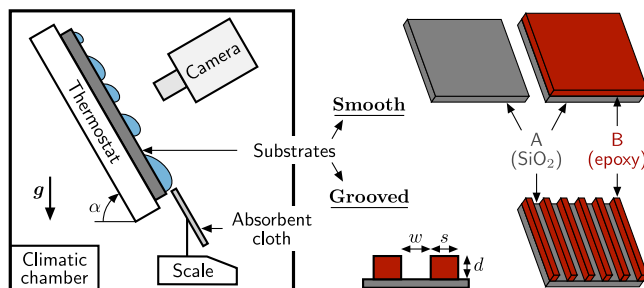

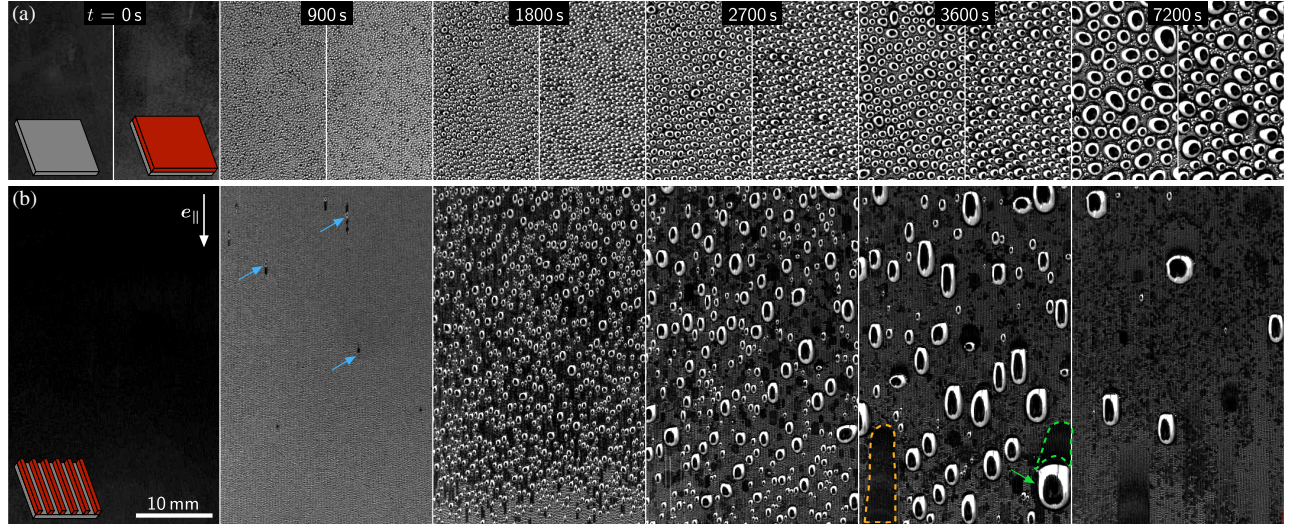FIG. 1. Schematic of the experimental setup and substrates.

098005-1

FIG. 2. Dew formation and drainage on (a) smooth surfaces (left: A; right: B) and (b) a grooved surface ($s = w = 100$ μm, $d = 65$ μm) under the same condensation rate $q = 45$ nm/s: The three surfaces are next to each other, cooled at the same temperature (4 ± 0.5 °C) and exposed to the same atmospheric conditions (33 ± 0.5 °C, $50 \pm 3\%$), with $\alpha = 30°$ (see also movie 1 in Ref. [27]). The drops appear as white hollow patches on the black background. Here, $e_\parallel$ indicates the grooves and steepest slope direction. The blue arrows indicate the first "large" drops formed by local overflow of the grooves. The green arrow points at a sliding drop. The dashed lines enclose areas recently wiped by drop shedding.

groove scale. At larger times ($t \gtrsim 900$ s), the spatial distribution of water on the grooved substrate becomes nonuniform over increasingly large distances, larger than both grooves and drop sizes. Fewer big drops emerge rapidly, and sliding eventually starts after typically 1 h, when a water height $qt \sim 0.15$ mm has condensed, whereas all of the dew is still retained at twice that time by both smooth surfaces [28]. Clearly, the shedding is not accelerated by the sole presence of materials A or B; it is a consequence of the texturization.

Figure 3 presents the mean projected area Σ of the five largest drops over a zone of 43×28 mm^2, for both grooved and smooth (A) substrates. On the smooth substrate, Σ increases quadratically with time (see Fig. 3 inset), as expected in the self-similar regime of dew formation, for which each drop with volume $\sim R^3$ results from the collection of a water height qt condensed over an area $\sim \Sigma \sim R^2$ [29]. On the grooved surface, growth is much faster, with a different scaling ($\Sigma \propto t^{3.5}$), revealing a specific growth mechanism. Nevertheless, the maximal value $\Sigma \simeq 13$ mm^2 reached at the onset of shedding is consistent with a simple force balance between pinning and gravity: Assuming, for simplicity, a semi-ellipsoidal shape with width $2R_\perp$, thickness $R_\perp$, and length $2R_\parallel$ gives $\rho g \sin \alpha 2\pi R_\perp^2 R_\parallel / 3 = \gamma \Delta \cos \theta 2R_\perp$, i.e., $\Sigma \equiv \pi R_\perp R_\parallel = 3\ell^2 \Delta \cos \theta / \sin \alpha \approx 10$ mm^2 (for contact angle hysteresis of both materials).

Growth mechanism and limits.—As on horizontal surfaces [14,16], small drops are confined to a single groove or plateau, but larger drops, forming when a groove locally overflows, span several grooves and remain

connected to liquid filaments partially filling the grooves. These filaments [not visible in the pictures of Fig. 2(b) but in the magnified views of Fig. 4(a); see also movie 2 in Ref. [27]] can extend over considerable lengths and mediate the coalescence between distant drops, as attested by the simultaneous shrinking and growth of drops
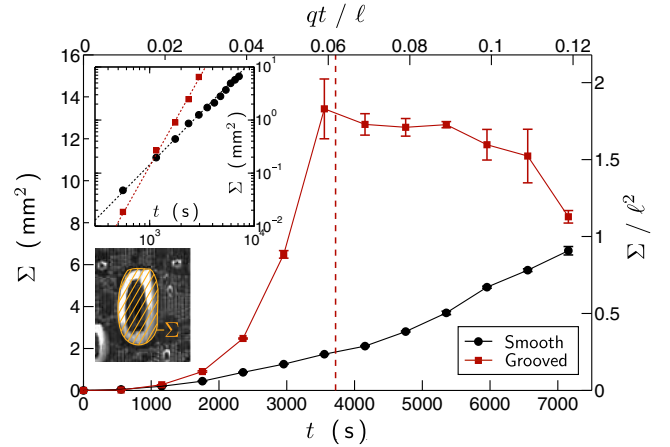

FIG. 3. Evolution of the largest drop sizes for the smooth (A) and grooved substrates shown in Fig. 2. Here, Σ is the mean projected area of the five widest drops over a surface of 43×28 mm^2 [same as in Fig. 2(b)]. The dashed line indicates the shedding onset time on the grooved surface; on the smooth substrate, no shedding occurs before the exogenous triggering by remote corner drops at $t \simeq 8000$ s, see Ref. [27]. The error bars show the standard deviation over the five drops. Inset: Same data in logarithmic scales. The black and red dashed lines are $\Sigma \propto t^2$ and $\Sigma \propto t^{3.5}$, respectively.
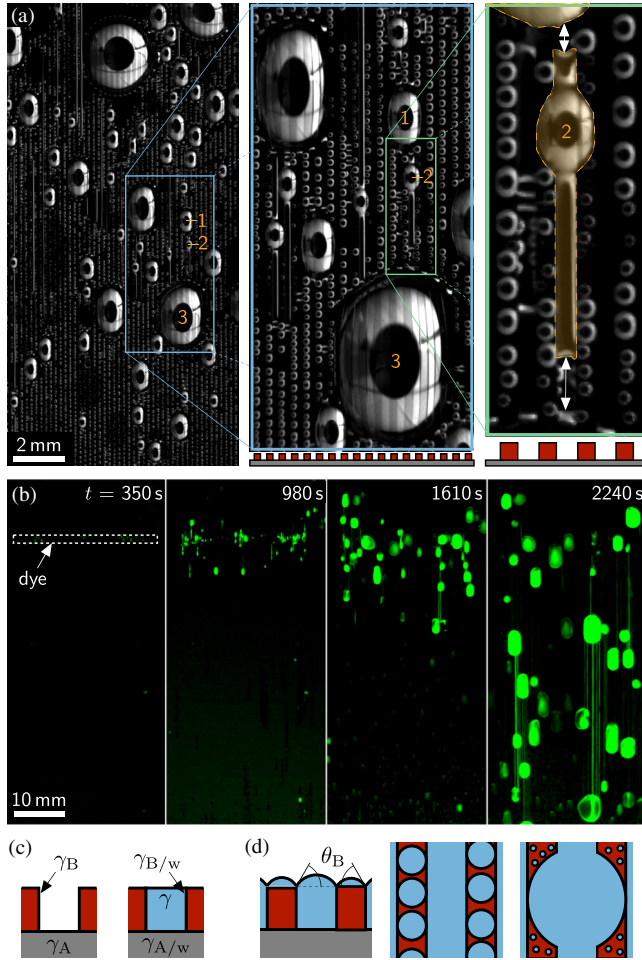
FIG. 4. Organization and interaction of dew drops on a grooved surface. (a) Close-up views of the condensation for a mean condensed water height $qt \simeq 50$ μm ($\alpha = 60°$, $w = s = 100$ μm, $d = 40$ μm, see also movie 2 in Ref. [27]). The textures location is indicated at the bottom. The orange dashed lines show the contour of drop "2", including the liquid filament to which it is connected. The arrows emphasize how close drop "2" is to coalesce with drops "1" and "3". (b) Long-range connection and coalescence between dew drops as evidenced by the motion of a fluorescent dye (see also movies 3 and 4 in Ref. [27]). The dashed line delineates the initial deposition area of the dye on the dry plate ($\alpha = 45°$, $w = d = 65$ μm, $s = 100$ μm, $q = 53$ mm/s). (c) Schematics for the groove imbibition criterion. (d) Schematics of the texture saturation and overflow considered for t_1 (left: cross section; right: top views just before and after t_1).

spanning the same grooves. This long-range interaction is evidenced more directly by seeding a thin region of a dry grooved substrate with a water-soluble fluorescent dye (Sigma-Aldrich Fluorescein). Upon condensation, the dye dissolves and fluoresces (under UV light), revealing the water transport [Fig. 4(b), see also movies 3 and 4 in Ref. [27]]: When a drop touches a filament connected to another drop, the smaller (or higher) drop drains into the larger (or lower) one due to pressure difference. The largest drops connect to more grooves and drains more water. This

promotes the growth of a few big drops, each of them concentrating water condensed over surfaces considerably larger than the typical area $\simeq R^2$ of the drop catchment basin on a smooth surface, which qualitatively explains the accelerated drop growth.

Long-range coalescence only occurs for grooves of sufficiently large aspect ratios d/w (independently of s); otherwise, the condensation logically resembles that on a smooth surface (see movie 5 in Ref. [27]). The critical ratio separating these two regimes is measured as $d/w = 0.34 \pm 0.09$ and 0.54 ± 0.11 for $\alpha = 30°$ and $45°$, respectively. It directly relates to the formation of groove-filling filaments, which requires that the imbibition of the grooves be thermodynamically favorable [30,31]. Indeed, when an imbibition front advances over a distance dx inside a small groove (w, $d \ll \ell$) connected to a large drop (with negligible Laplace pressure), the free energy of the groove and filament system varies as $dF/dx = w(\gamma + \gamma_{A/w} - \gamma_A) + 2d(\gamma_{B/w} - \gamma_B) = \gamma[w(1 - \cos\theta_A) - 2d\cos\theta_B]$ [see notations in Fig. 4(c)]. Groove-filling imbibition ($dF/dx < 0$), involving the advancing contact angles, thus occurs only if

$$\frac{d}{w} > \frac{1 - \cos\theta_A}{2\cos\theta_B} \simeq 0.52. \tag{1}$$

Small deviations from Eq. (1) may originate from the curvature of the filaments surface allowed by contact line pinning at the groove edges [30,32], which is not considered in Eq. (1) but accommodates pressure variations experienced during coalescence events. Although the actual filling-up of the grooves may involve dynamical wetting motions associated with droplet coalescence as well as the groove wedges imbibition stability in the presence of wetting hysteresis, Eq. (1) is found to compare well with the experimental thresholds.

Dew shedding.—To quantify the influence of the grooves [above the threshold given by Eq. (1)], we varied their dimensions and measured the quantity of water draining as a function of time. A cloth resting on a scale and stretched 0.2 mm above the bottom of the substrate was used to absorb and weigh the sliding drops (Fig. 1).

Figure 5 presents the condensed volume v (expressed in L/m^2 or mm) collected for substrates having the same groove width and depth ($w = 100$ μm, $d = 65$ μm) but different spacings s. Each step increase in v denotes a collection event on the cloth. Despite an equal condensation rate q, the shedding onset time t_s (which is identical to the first collection event time within a few seconds) depends significantly on s. Beyond t_s, the average rate of collection is close to q: Water storage by the substrate remains constant ($\approx qt_s$), and the process of condensation and drainage is steady. Then, on first estimate, t_s determines the whole water recovery curve for a given condensation rate q. In the following, we focus on qt_s, i.e., the
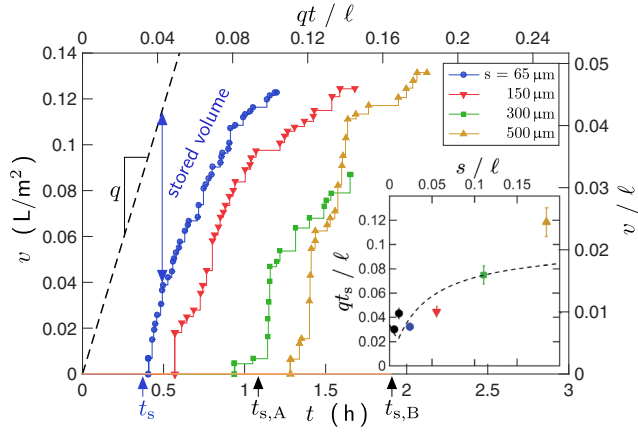
FIG. 5. Main panel: Condensation volume collected at the substrate lower edge versus time for grooves with increasing spacing s (symbols) and identical width and depth ($w = 100$ μm, $d = 65$ μm, $\alpha = 45°$, $q = 65$ nm/s). Each step denotes a drop collection event. The dashed line shows the mean condensed water volume. "Stored volume" and t_s indicate (for $s = 65$ μm) the condensate stored on the substrate and the shedding onset time at which the first drop starts to slide, respectively. Note that $t_{s,A}(\simeq 1.1$ h) and $t_{s,B}(\simeq 1.9$ h) indicate the shedding times expected for surfaces A and B (see Ref. [27]). Insert: Shedding time versus groove spacing, in dimensionless coordinates. The dashed line is Eq. (4).

smallest dew volume that can be collected for any low condensation rate process, including natural dew. As shown in the insert of Fig. 5, qt_s more than triples when s is increased from 65 μm to 500 μm. To rationalize the dependence of qt_s on the grooves geometry, we consider the two necessary conditions for drop shedding. First, some grooves must overflow to form large drops and initiate long-range coalescence. Second, the coalescences must concentrate enough water to form drops which depin from the substrate. These conditions define two times, t_1 and t_2, respectively.

The time t_1 is typically set by the volume of water required to saturate the texture over a period of $w + 2s$, since the first grooves to overflow collect water from their two adjacent plateaus, as sketched in Fig. 4(d) [see Fig. 2 at 900 s and drop '2' in Fig. 4(a)]. Thus, t_1 reads, with $\theta = (\theta_{a,B} + \theta_{r,B})/2$,

$$qt_1 \simeq \frac{wd + \frac{\theta - \sin\theta\cos\theta}{4\sin^2\theta}w^2 + \frac{\pi}{16}\frac{2 - 3\cos\theta + \cos^3\theta}{\sin^3\theta}s^2}{w + 2s}. \quad (2)$$

The three terms in the numerator (derived in Ref. [27]) are, respectively, the volume (per unit length) inside the groove, above the groove and on top of the plateaus, where the saturation corresponds to spherical cap drops of base radius $s/2$ with a one-dimensional random packing fraction ≈ 0.75.

The time t_2 is set by the depinning condition $\rho g\Omega \sin\alpha \sim 2R_\perp\gamma\Delta\cos\theta_B[s/(w + s)]$, where Ω and $2R_\perp$ are, respectively, the critical drop volume and drop width (in the direction perpendicular to the grooves), and the factor $[s/(w + s)]$ accounts for the pinning of the drops on top of the plateaus. Indeed, some water remains in the grooves when a drop slides, and the triple line is limited to the plateaus [14]. Yet, the main influence of the grooves is to extend the catchment basin of large drops by long-range coalescence. Observation suggests that the captation length perpendicular to the grooves remains $\sim R_\perp$, whereas the one parallel to the grooves, denoted as L_{capt}, relates to the much longer filament length and is either limited by the grooves length L itself or by the range of the capillary imbibition of the grooves under the typical Laplace pressure γ/w that its meniscus can accommodate. This reads $L_{capt} = \min\{L, \beta_1[\ell^2/(w\sin\alpha)]\}$, with β_1 a numerical parameter accounting for the effective imbibition length. Assuming that each of the largest drops concentrates a constant fraction β_2 of the water from its catchment basin gives $\Omega \sim \beta_2 2R_\perp L_{capt}qt_2$, i.e.,

$$qt_2 = \frac{1}{\beta_2}\frac{\Delta\cos\theta_B}{\sin\alpha}\frac{s}{w + s}\frac{\ell^2}{L_{capt}}. \quad (3)$$

The two processes underlying t_1 and t_2 being essentially concomitant, the onset shedding time is expected to be limited by the longest one, according to

$$qt_s = \max(qt_1, qt_2). \quad (4)$$

As Fig. 6 shows, Eq. (4) captures the shedding time provided that $\beta_1 \simeq \beta_2 \simeq 0.3$. The data show some scatter (within typically $\pm 30\%$) due to the small number of sliding drops, but they follow both the magnitude and the trend of
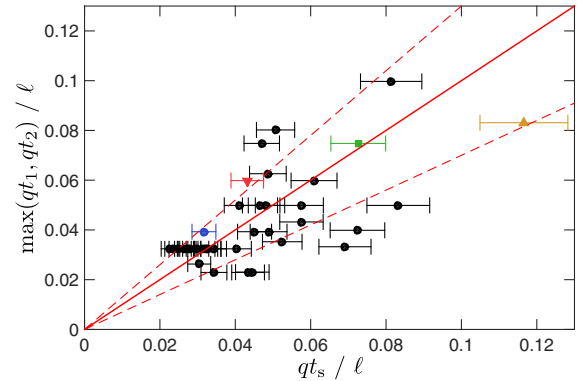

FIG. 6. Comparison of Eq. (4) with all the experimental data for which long-range coalescence is observed ($15 \leq w \leq 500$ μm, $15 \leq s \leq 500$ μm, $15 \leq d \leq 150$ μm, $2 \leq L \leq 7$ cm, $15° \leq \alpha \leq 90°$). The red solid line is the theoretical prediction (with $\beta_1 = \beta_2 = 0.3$). The dashed lines show the $\pm 30\%$ spread. Colors hold for the data of Fig. 5.

the prediction all over the large range of parameters explored ($15\,\mu m < w$, $s < 500\,\mu m$, $15\,\mu m < d < 150\,\mu m$, $2\,cm < L < 7\,cm$, and $15° < \alpha < 90°$). The fitting parameters β_1 and β_2 are both of order one and smaller than one, consistent with the constraints that the catchment basin is limited by capillary imbibition and can only be partially drained.

Conclusion.—Laboratory experiments show that appropriate grooving of a tilted surface hastens dew shedding significantly. This effect is due to an accelerated coarsening of dew drops, with a smaller influence of drop pinning and no modification of the condensation rate. It involves an oriented long-range coalescence mechanism mediated by water filaments, whose formation demands submillimetric grooves ($\ll \ell$) with large depth-to-width ratio and partially wetted materials as expressed by Eq. (1). These findings suggest that condensates with equivalent heights as small as the groove dimensions could be collected by gravity. Provided that large-scale and resilient micro-grooving can be made affordable, they open promising opportunities for considerably improving the collection of small volumes of condensates, such as natural dew water harvesting. In addition, this study may help us to understand how grooves can be used to accelerate drainage and passively direct water on heat exchange surfaces [33], fog collecting materials [34], and open microfluidic systems [35].

---

[*]daniel.beysens@espci.fr

[1] World Health Organization, *Global Water Supply and Sanitation Assessment 2000 Report* (Geneva, Switzerland, 2000).

[2] P. H. Gleick, Science **302**, 1524 (2003).

[3] M. M. Mekonnen and A. Y. Hoekstra, Sci. Adv. **2**, e1500323 (2016).

[4] R. V. Wahlgren, Water Res. **35**, 1 (2001).

[5] H. Kim, S. R. Rao, E. A. Kapustin, L. Zhao, S. Yang, O. M. Yaghi, and E. N. Wang, Nat. Commun. **9**, 1191 (2018).

[6] I. Lekouch, M. Muselli, B. Kabbachi, J. Ouazzani, I. Melnytchouk-Milimouk, and D. Beysens, Energy **36**, 2257 (2011).

[7] W. Wells, *An Essay on Dew and Several Appearances Connected with It* (Longmans, London, 1866).

[8] J. L. Monteith, Q. J. R. Meteorol. Soc. **83**, 322 (1957).

[9] D. Beysens and C. M. Knobler, Phys. Rev. Lett. **57**, 1433 (1986).

[10] M. Tomaszkiewicz, M. A. Najm, D. Beysens, I. Alamedine, and M. El-Fadel, Environmental reviews **23**, 425 (2015).

[11] D. Beysens, I. Milimouk, V. Nikolayev, M. Muselli, and J. Marcillat, J. Hydrol. **276**, 1 (2003).

[12] C. Furmidge, J. Colloid Sci. **17**, 309 (1962).

[13] C. W. Extrand and A. N. Gent, J. Colloid Interface Sci. **138**, 431 (1990).

[14] R. D. Narhe and D. A. Beysens, Phys. Rev. Lett. **93**, 076103 (2004).

[15] A. Lee, M.-W. Moon, H. Lim, W.-D. Kim, and H.-Y. Kim, Langmuir **28**, 10183 (2012).

[16] Y. Zhong, A. M. Jacobi, and J. G. Georgiadis, Int. J. Heat Mass Transfer **57**, 629 (2013).

[17] A. Ghosh, S. Beaini, B. J. Zhang, R. Ganguly, and C. M. Megaridis, Langmuir **30**, 13103 (2014).

[18] D. Seo, C. Lee, and Y. Nam, Langmuir **30**, 15468 (2014).

[19] M. K. Chaudhury, A. Chakrabarti, and T. Tibrewal, Extreme Mech. Lett. **1**, 104 (2014).

[20] K.-C. Park, P. Kim, A. Grinthal, N. He, D. Fox, J. C. Weaver, and J. Aizenberg, Nature (London) **531**, 78 (2016).

[21] Y. Jin, L. Zhang, and P. Wang, Global Challenges **1**, 1700019 (2017).

[22] M. M. Garimella, S. Koppu, S. S. Kadlaskar, V. Pillutla, Abhijeet, and W. Choi, J. Colloid Interface Sci. **505**, 1065 (2017).

[23] F. T. Malik, R. M. Clement, D. T. Gethin, W. Krawszik, and A. R. Parker, Bioinspiration Biomimetics **9**, 031002 (2014).

[24] F. T. Malik, R. M. Clement, D. T. Gethin, M. Kiernan, T. Goral, P. Griffiths, D. Beynon, and A. R. Parker, Phil. Trans. R. Soc. A **374**, 20160110 (2016).

[25] Z. Pan, W. G. Pitt, Y. Zhang, N. Wu, Y. Tao, and T. T. Truscott, Nat. Plants **2**, 16076 (2016).

[26] D. Xia, L. M. Johnson, and G. P. López, Adv. Mater. **24**, 1287 (2012).

[27] See Supplemental Material at http://link.aps.org/supplemental/10.1103/PhysRevLett.122.098005 which provides five illustrating movies with their descriptions, together with the derivations of the water height in one saturated groove, and the onset time of shedding on a smooth substrate.

[28] Note that on the smooth surface, drop sliding is eventually triggered by exogenous side effects at $qt \sim 0.4$ mm; see Ref. [27].

[29] J.-L. Viovy, D. Beysens, and C. M. Knobler, Phys. Rev. A **37**, 4965 (1988).

[30] R. Seemann, M. Brinkmann, E. Kramer, F. Lange, and R. Lipowski, Proc. Natl. Acad. Sci. U.S.A. **102**, 1848 (2005).

[31] J. Berthier, K. A. Brakke, and E. Berthier, Microfluid. Nanofluid. **16**, 779 (2014).

[32] S. Herminghaus, M. Brinkmann, and R. Seemann, Annu. Rev. Mater. Res. **38**, 101 (2008).

[33] L. Liu, A. M. Jacobi, and D. Chvedov, J. Micromech. Microeng. **19**, 035026 (2009).

[34] M. A. K. Azad, D. Ellerbrok, W. Barthlott, and K. Koch, Bioinspiration Biomimetics **10**, 016004 (2015).

[35] P. Comanns, G. Buchberger, A. Buchsbaum, R. Baumgartner, A. Kogler, S. Bauer, and W. Baumgartner, J. R. Soc. Interface **12**, 20150415 (2015).